AD_____

Award Number: DAMD17-96-1-6289

TITLE: High Temperature Superconductor RF Probes for Breast Cancer Research

PRINCIPAL INVESTIGATOR: Paul C. Wang, Ph.D.

CONTRACTING ORGANIZATION: Howard University
Washington, DC 20059

REPORT DATE: October 2000

TYPE OF REPORT: Annual

PREPARED FOR: U.S. Army Medical Research and Materiel Command
Fort Detrick, Maryland 21702-5012

REPORT DOCUMENTATION PAGE

Form Approved
OMB No. 074-0188

1. AGENCY USE ONLY (Leave blank)	2. REPORT DATE	3. REPORT TYPE AND DATES COVERED
	October 2000	Annual (20 Sep 99 - 19 Sep 00)

4. TITLE AND SUBTITLE
High Temperature Superconductor RF Probes for Breast Cancer Research

5. FUNDING NUMBERS
DAMD17-96-1-6289

6. AUTHOR(S)
Paul C. Wang, Ph.D.

7. PERFORMING ORGANIZATION NAME(S) AND ADDRESS(ES)
Howard University
Washington, DC 20059

E-MAIL:
pwang@howard.edu

8. PERFORMING ORGANIZATION REPORT NUMBER

9. SPONSORING / MONITORING AGENCY NAME(S) AND ADDRESS(ES)
U.S. Army Medical Research and Materiel Command
Fort Detrick, Maryland 21702-5012

10. SPONSORING / MONITORING AGENCY REPORT NUMBER

11. SUPPLEMENTARY NOTES

12a. DISTRIBUTION / AVAILABILITY STATEMENT
Approved for public release; distribution unlimited

12b. DISTRIBUTION CODE

13. ABSTRACT ***(Maximum 200 Words)***

For the fourth year there has been a significant improvement of the in vivo spectroscopy study. An improved cell perfusion system was constructed. Using the improved perfusion system the duration of the cell metabolism studies has been extended to longer than 6 days, which is much longer than the previously reported 14 hours. This long and stable study significantly improved the signal-to-noise ratio of the NMR spectrum. Many phosphorus metabolites have been identified including: phosphoethanolamine (PE), phosphocholine (PC), inorganic phosphate (Pi), glycerophosphoethanolamine (GPE), glycerophosphocholine (GPC), phosphocreatine (PCr), γ-adrinophosphate (γ-ATP), α-adrinophosphate (α-ATP), diphosphodiester (DPDE), and β-adrinophosphate (β-ATP). Some of the entwined peaks, particularly in the PE/PC, GPE/GPC, and intra- and extra-cellular Pi regions, can be separated. With the improved NMR perfusion system four MCF7 breast cancer cells drug sensitivity studies were conducted. Drugs with different concentrations were perfused through the NMR tube. The concentrations of the high energy phosphates such as ATP and PCr decreases and the intracellular Pi increases. The GPE and GPC shows a slight increase initially and a decrease later. Changes in phosphorus metabolic activity indicate that the cells were under stress when first exposed to the drug. Later, the toxic effects of the drug overwhelmed the cells.

14. SUBJECT TERMS
Breast Cancer, magnetic resonance spectroscopy (MRS), magnetic resonance imaging (MRI), cancer cell metabolism, high temperature superconductor

15. NUMBER OF PAGES
27

16. PRICE CODE

17. SECURITY CLASSIFICATION OF REPORT	18. SECURITY CLASSIFICATION OF THIS PAGE	19. SECURITY CLASSIFICATION OF ABSTRACT	20. LIMITATION OF ABSTRACT
Unclassified	Unclassified	Unclassified	Unlimited

Table of Contents

V. Introduction

Conventional mammography has been shown to play an important role in detection and staging of breast cancer in older women. For younger women who frequently have radiodense breast tissue or women with silicon implants, rendering breast cancer diagnosis with conventional mammography is problematic. When mammographic findings and clinical findings concur regarding the possibility of a lesion being malignant, usually a fine-needle aspiration biopsy will be performed for definitive diagnosis. The false positive rate is high; only 20-30% of lesions suspicious for cancer at mammogram are actually positive for cancer at biopsy. In general, mammography is limited to detect a tumor several millimeters or larger in size. Because of difficulty with early detection, clinicians are sometimes limited to treat larger size cancers, which in many cases have already metastasized. Accurate definition of tumor size, number, and margins is highly critical in the clinical determination of conservation treatment versus mastectomy. A role exists for an imaging method that can improve sensitivity for detection of small lesion and to improve the specificity for better staging of the disease. To provide the best chance of overall survival, breast cancers need to be accurately staged for systemic treatment and optimal conservation surgery. Traditionally, the gold standards for such assessments are clinicopathological staging and histopathological typing and grading of malignancy. In the classical histopathological approach problems exist inherently, predominantly, the accuracy of the initial biopsy procedure and the variable skills applied to its histological assessment. Development of a new modality to remove sampling errors, improve specificity and produce a grading of tissues that relates to establish biological criteria would be very useful.

Over the last few years, magnetic resonance imaging (MRI) and spectroscopy (MRS) have emerged as one of the most promising clinical tools to fill the gap between clinical needs and information obtained by conventional breast imaging and pathological methods. Preliminary results indicate that MRI may be more sensitive than conventional x-ray mammography in detecting small lesions. Cancers have typical metabolic characteristics in ^{31}P and ^{1}H MRS including high levels of phospholipid metabolites and a cellular pH more alkaline than normal. Although these alone are not unique for cancer they are very useful diagnostic information in appropriate clinical settings. MRS is capable of distinguishing benign and malignant lesions in a particular anatomical site and to be a specific diagnostic discriminant in a particular situation. It has been demonstrated to be useful to improve the specificity of the MR imaging of breast. Some metabolic characteristics appear to be prognostic indices and correlate well with the response of treatment. The improvement of specificity will reduce the number of biopsies performed to confirm false-positive mammographic findings and more effectively assess the results of treatment. Many of these progresses are based on the advances of nuclear magnetic resonance (NMR) studies of perfused breast cancer cells and tumor-bearing animal models. One of the major limitations of the application of NMR methods both in vitro and in vivo is its low sensitivity. The sensitivity determines the ultimate cancer detection capability and the resolution in image and in spectrum. In this study, a high temperature superconductor (HTS) working at very low temperature will be used to reduce electronic noise and significantly improve the sensitivity of detection. It will dramatically increase the sensitivity and improve the resolutions. The improvement will be verified by comparing the sensitivity with that of a conventional probe.

The improvement of detection sensitivity will provide a more accurate diagnosis, and it may become possible for early prediction of tumor response to therapy. The probes will be constructed with $YBa_2Cu_3O_7$ material and tested in two well defined experiments: an in vitro cell metabolism study on a 9.4 T spectrometer and an in vivo tumor bearing animal study on a 4.7 scanner. In the cell metabolism study, the breast cancer cell line MCF7 and its variants will be studied in terms of characteristic differences of their ^{31}P spectra during growth phase and under effects of Tamoxifen. In the in vivo animal study, MCF7 cells and its variants will be grown as xenografts on nude mice. The differences of 31P spectra during progress of tumor and responses to Doxorubicin and Tamoxifen will be studied. The high-resolution proton imaging experiments of vasculature of tumor will be conducted using both conventional copper probe and the proposed HTS probes.

VI. Body

In the first year of the project, the design of self-resonant probes for high-resolution NMR has been completed. The receiver coil uses thin-film, high temperature superconductor (HTS), $YBa_2Cu_3O_7$. The transmitter coil is a standard room-temperature coil. The probe is designed to fit either a 9.4 T machine for in vitro cell study or a 4.7 T machine for animal study. The coils are detachable so that different coil can be substituted in and out of the different machines and for different nuclei. Three identical cell perfusion apparatus for the NMR study of breast cancer cell metabolism have been constructed and tested. The apparatus was tested using known standard compounds. To study the metabolism of breast cancer cells for an extended period of time, the cells are continuously perfused with nutrients. During perfusion, the breast cancer cells are restrained in agarose gel-thread matrices. A protocol for making agarose gel-thread matrices containing MCF7 breast cancer cells is established. Besides the above-mentioned tasks, some of the infrastructure and preparation works necessary for conducting the proposed research have been accomplished including relocation of a 400 MHz machine and renovation of laboratories.

In the second year of this project, we have fabricated and tested a HTS coil, as well as, studied the ^{31}P spectroscopic differences of MCF 7 cells and its variants and their responses to Tamoxifen and Doxorubicin. Based on the test done at 77 ^{0}K, the HTS coil has a resonance frequency 401.6 MHz and the Q value for the coil is 650. This is better than we expected in the design. Since the coil is going to be mounted in the cryostat on a sapphire substrate and cooled below 40^0 K, the Q should increase further. We have studied the differences in the ^{31}P NMR spectroscopic profiles for drug sensitive MCF7 cancer cells and their multidrug resistant variant MCF7/ADR cells. The cells are embedded in agarose gel threads and perfused with growth medium during the NMR studies. Many detailed phosphorus metabolites have been identified. There may be some subtle differences in the spectra of the two cell lines. However, the differences are not conclusive using the conventional probe. We have successfully demonstrated drug sensitive MCF7 cells, which were dramatically affected by 2 μM Doxorubicin within two hours perfusion and not responsive to Tamoxifen up to 12 hours. In contrast, 2 μM Doxorubicin was without any effect on multidrug resistant MCF7/ADR cells and the ^{31}P NMR spectrum did not differ appreciably after addition of Doxorubicin. In order to have a highest S/N in the in vivo studies, a great deal of efforts has

been made to ensure a reliable NMR system and a contamination free cell culture environment. The scan parameters are optimized. The magnetic field drift during the long acquisition time is negligible. All the potential cell contamination sources are eliminated.

In the third year, we concentrated on the in vivo animal study. The MCF7 wild type human breast cancer cells and its drug resistant variants were grown as solid tumor xenographs in athymic nude mice as the animal model. This in vivo animal study was a continuation of our previous in vitro cell study. The results from the animal model will be used to confirm whether the differences seen in vitro are also observed in the in vivo spectra obtained for the tumors growing in nude mice. The in vivo NMR imaging and spectroscopy studies of the solid tumor have been providing information regarding (i) heterogeneity and microvasculature of tumor, (ii) energy metabolism, (iii) tumor pH, (iv) tumor hypoxia, (v) observed predictive response to antiestrogens and Doxorubicin even before regression by tumormeter measurements. Besides this in vivo animal study, we also have completed the integration of the Oxford Spectrostate cryostat with the HTS probe. The whole system includes HTS coil, mounting facilities, the fine tuning paddle and a copper impedance matching loop and the preamp.

In the third year, we also have procured the specialized cryo-valves, low temperature components and Oxford cryostat. The HTS probe was assembled with the cryostat at Quantum Magnetics Inc (subcontractor). The whole HTS probe underwent a final evaluation for its operation characteristics. In this year the research effort was concentrated on the in vivo localized spectroscopy and micro-imaging studies. A localized spectroscopy technique ISIS (image-selected in vivo spectroscopy) technique has been implemented and tested. The intended selected volume was well defined. To study the progress of tumor a series of the in vivo ^{31}P spectra were taken from MCF7/ADR drug resistant tumor on 4, 6, 8, and 12 days after cell implantation. The spectra clearly showed the gradual decreases of phosphocreatine and ATP. The spectra also showed the increase of inorganic phosphate. The potential malignant markers such as phosphomonoester and phosphodiester signals were weak. This weak signal detection may be improved by replacing the conventional RF probe with the proposed HTS probe. The spectra from the non-involved control leg demonstrated no metabolic changes during this period. The consistent spectral intensities also demonstrated the consistency of the NMR machine. The results from these in vivo ^{31}P spectroscopic studies were similar to the results from the in vitro cell studies. The signal-to-noise ratio of the in vivo animal studies was better. This was primarily due to more cells involved in the in vivo studies. In the third year, we have also studied the small blood vessels of mouse using NMR microscopic imaging technique. The in-plane spatial resolution was 30 μm. A series of high quality detailed images revealed the fine microscopic structures of mouse capillaries.

For the forth year, we continued the in vivo spectroscopy study. We had constructed an improved cell perfusion system (Figure 1). The improved cell perfusion system contained both a negative pressure and a positive pressure part before and after the pump. These negative and positive pressure parts helped with the removal of air bubbles in the medium. They also served as reservoirs to trap the air. An air bubble trapped in the NMR tube would cause magnetic field inhomogeneity and, consequently, degrade the quality of the spectrum. Using the improved perfusion system, the proposed cell metabolism studies could be extended

to a much longer time, more than 6 days. In the previous study, the experiment could only run up to 14 hours. With this improved perfusion system, many time consuming experiments can be performed more reliably and the signal-to-noise ratio has been dramatically improved.

MCF7/WT (wild type) breast cancer cells (~10^8) were grown as conventional monolayers and harvested as single cell suspensions, which were then embedded in agarose gel threads. These cells embedded in agarose threads were transferred to a NMR tube and then perfused with culture medium using the new perfusion system. The details of cell culture and making agarose gel-thread matrices were reported in previous years. Figure 2 shows an improved NMR spectrum. Phosphorus metabolites can be easily identified including phosphoethanolamine (PE, 4.21 ppm), phosphocholine (PC, 3.66), inorganic phosphate (Pi, 2.47), glycerophosphoethanolamine (GPE, 0.92), glycerophosphocholine (GPC, 0.37), phosphocreatine (PCr, -2.61), γ-adrinophosphate (γ-ATP, -5.05), α-adrinophosphate (α-ATP, -10.15), diphosphodiester (DPDE, -10.78, -12.53), and β-adrinophosphate (β-ATP, -18.70). The spectrum is an accumulation of 1800 transients and the repetition time is 2 seconds. The line broadening used is 10 Hz. The signal-to-noise ratio is significantly better than the results in the previously reported (see the insert). The line width of the γ-ATP peak is 50 Hz. The ^{31}P NMR spectrum can be deconvoluted. Each individual component of phosphorus metabolites can be separated from the spectrum (Figure 3). The individual peak-height and the integral under the peaks can be calculated and listed as in the inserted table. The differences between the original spectrum and the fitted curve shown on the bottom of the figure indicate the decomposition of the peaks is complete.

Since the signal-to-noise ratio of the NMR spectrum is usually low, sometimes a long scan time is needed. This long data acquisition time prevents some fast changing experiments such as drug effects on the metabolism of breast cancer cells. With the improved perfusion system, long term in vivo study becomes feasible. Figure 4 shows a long term in vivo ^{31}P NMR spectroscopy study of MCF7 breast cancer cells. A serious of ^{31}P spectra over 5 days was obtained. Each spectrum is an accumulation of 3 hours, 5370 transients and 2 seconds repetition time. The line broadening is 10 Hz. Only every other spectrum is shown in the Figure 4. The changes of each phosphorus metabolites can be easily studied. During this time, PC, GPE and GPC increases while other phosphorus metabolites stay constant. Changes of individual phosphorus metabolites of MCF7/WT (wild type) cells over first 72 are carefully studied. Figure 5A shows the concentrations of 6 out of 11 phosphorus metabolites: PE, PC, GPC and DPDE. Figure 5B shows the relative intensities of these metabolites as functions of time. During the first 72 hours, GPE and GPC continuously increase while PE and DPDE remains constant. The PC peak increases initially and it approaches a plateau later. The increases of GPE and GPC indicate the cell proliferation. Figure 6A shows the concentrations of another five phosphorus metabolites α-ATP, β-ATP, γ-ATP, PCr, and Pi. Figure 6B shows the relative intensities as functions of time. During the course of study, ATP and Pi continuously grow and PCr remains constant.

With the improved NMR perfusion system four drug sensitivity studies were conducted using iodoacetamide, rotenone and barbital with different concentrations. 10^8 MCF7/WT breast cancer cells embedded in the agarose gel were first perfused with growth medium. After the system is stabilized (~2 hours after perfusion with medium), a series of

forty-two one-hour ^{31}P NMR spectra were taken. Each spectrum contains 1700 transients with 1 second repetition time. After 17 hours baseline study, 1mM iodoacetamide (or 0.5 mM iodoacetamide, or 1 mM rotenone, or 0.5 mM barbital) was added in the perfused medium. Figure 7 and Figure 8 shows the phosphorus metabolites concentrations plotted as functions of time. Six metabolites are in Figure 7 and the other five metabolites are in Figure 8. Figure 7A shows the absolute concentration changes of the PE, PC, GPE, GPC and DPDE. Figure 7B shows the relative concentration changes of these metabolites to the concentrations at the beginning of the study. After perfusion with iodoacetamide, PE increases dramatically and then decreases. GPE and GPC show slightly increases initially and decreases afterwards. DPDE shows continuous decreases. In Figure 8, it shows the other five phosphorus metabolites: α-ATP, β-ATP, γ-ATP, intra- and extra- cellular Pi. After perfusion with iodoacetamide, ATP increases slightly and then decreases. The rates of decreasing GPE, GPC, DPDE and ATP depend on the concentrations of iodoacetamide. Iodoacetamide is an inhibitor of the electron transport chain and consequently it will change the respiratory states of the cells. While the concentrations of high-energy phosphates decreases, the intracellular Pi continuously increases. A new extracellular Pi peak appears immediately after the drug perfusion and the concentration of the extracellular Pi increases for few hours before it disappears due to the perfusion. The ability of detection of extracellular Pi and separated from the intracellular Pi is new and exciting.

The NMR T1 relaxation times of all the phosphorus metabolites of MCF7 breast cancer cells were measured with the improved NMR perfusion system. Since some of the T1 of the phosphorus metabolites are long, the T1 measurement is difficult. It requires a long measurement time. The T1 measurement of the phosphorus metabolites becomes feasible only with the improved perfusion system. A saturation recovery technique has been used for the T1 measurement in this study (Figure 9). A series 16 RF pulses flips the magnetization to horizontal plane first. It follows by a 90^0 pulse and the data acquisition. The measured T1 relaxation times for each phosphorus metabolites are listed in the table in the Figure 9. The T1 values vary from 0.38 seconds for β-ATP to 12 seconds for GPE.

Key Research Accomplishments

The accomplishment in the forth year is highlighted in the following Statement of Work.

I. Probe Design (10/96-09/98, 24 months)

162 MHz ^{31}P Probe for Cell Metabolism Study on 9.4 T machine

1. Detail the design of HTS probe for 9.4 T NMR machine (complete)
2. Procure specialized cryo-valves and low temperature mechanical and electrical components (complete)
3. Order cryogenic preamplifier and test its specifications (complete)
4. Fabricate the components of HTS probe (complete)
5. Assemble the HTS probe (complete)
6. Construct conventional copper probe for comparison (complete)
7. **Evaluate components and test the operation characteristics of HTS probe. Determine**

the SNR gain as function of temperature on conductive and non-conductive samples (in progress)

II. Cell Metabolism Study (02/97-07/98, 18 months)

The cell metabolism study and in vivo animal study have begun. The initial phase of the studies will be using conventional room temperature probes. It will serve as comparison studies.

1. **To construct the perfusion apparatus and setup the perfusion experiment (complete)**
2. **Obtain ^{31}P spectra of MCF7, MCF7/III, MCF7/LCC2 and MCF7/LY2 in agarose gel in order to compare the SNR improvement by HTS probe. (in progress)**
3. **To determine the lowest cell density which still can have a good SNR in a reasonable acquisition time. A study of MCF7 cell proliferation in Matrigel from a low starting cell density will be conducted. (complete)**
4. To study of the effect of Tamoxifen and growth effectors on these breast cancer cell lines. (complete)

III. In Vivo Animal Study (04/98-09/00, 30 months)

1. **To obtain in vivo ^{31}P MRS spectra during growth and progression of MCF-7, MCF-7/MIII, MCF-7/LCC2 and MCF-7/ADR tumors in athymic nude mice using the conventional probe as well as the HTS probe. Following groups will be studied: (in progress)**
   (i) Normal athymic nude (10 animals).
   (ii) Mice with MCF-7 tumors in one leg (10 animals).
   (iii) Mice with MCF-7/ADR tumors in one leg (10 animals).
   (iv) Mice with MCF-7/LCC2 tumor in one leg (10 animals).
   (v) Mice with MCF-7/MIII tumor in the other leg (10 animals).

2. **To study the ^{31}P MRS of the different tumors at different times after treatment with Doxorubicin and Tamoxifen used singly or in combination. (in progress)**
   To study Tamoxifen:
   (i) Mice with MCF7 tumor in one leg and MCF7/MIII tumor in the other leg (15 animals).
   (ii) Mice with MCF7 tumor in one leg and MCF7/LCC2 tumor in the other leg (15animals).
   (iii) Mice with MCF7/MIII tumor in one leg and MCF7/LCC2 tumor in the other leg (15 animals).
   (iv) Mice with MCF-7 tumor in one leg and MCF-7/ADR tumor in the other leg (15animals).
   To study Doxorubicin:
   (I) Mice with MCF-7 tumor in one leg and MCF-7/ADR tumor in the other leg, but treated with one or three cycles of Doxorubicin treatment (30 animals).
   (ii) Same as group (I) but treated with one or three cycles of Doxorubicin in combination with Tamoxifen (30 animals).

3. **Utilize a high resolution MRI and a gradient-echo dynamic contrast enhancement technique to examine capillary densities in tumors and the relative permeability or leakiness of the capillaries in the different tumors before and during the different stages of treatment with Tamoxifen and/or Doxorubicin. These will be done at the same time when task (2) is performed. (same time as (2)) (in progress)**

Reportable outcomes

1. An improved perfusion system has been constructed. The signal-to-noise ratio of the in vivo ^{31}P spectrum has shown significant improvement. The in vivo study can be extended from 14 hours to longer than 6 days. Due to this improved capability of long in vivo study, the drug sensitivity of MCF7 breast cancer cells has been studied more accurately in time with much lower drug concentrations.
2. The quality of the ^{31}P spectrum has shown dramatic improvement. The linewidth of the ^{31}P peaks is in the order of 50 Hz, which is significantly better than the previously reported ~100 Hz. All the phosphorus metabolites peaks are well separated in the spectrum. Consequently, the concentrations of each individual phosphorus metabolites have been measured more accurately. The changes of phosphorus metabolites concentrations have been studied in every hour and over 6 days.
3. Two postdoctoral fellows, Dr. Yuling Chi and Dr. Jienwei Zhou, and one MD/PhD student Mr. Emmanuel Agwu are supported by this grant.
4. Two U.S. Army training grants have been received based on this research:

- "MR Sensitivity Improvement Using High Temperature Superconductor for RF Probe" (DAAG55-98-1-0187)
- "A Training Program in Breast Cancer Research Using NMR Techniques" (DAMD-17-00-1-0291)

VII. Conclusions

For the fourth year there has been a significant improvement of the in vivo spectroscopy study. We have constructed an improved cell perfusion system. Using the improved perfusion system the duration of the cell metabolism studies has been extended to longer than 6 days, which is much longer than the previously reported 14 hours. This long and stable study significantly improved the signal-to-noise ratio of the NMR spectrum. Many phosphorus metabolites have been identified including: phosphoethanolamine (PE), phosphocholine (PC), inorganic phosphate (Pi), glycerophosphoethanolamine (GPE), glycerophosphocholine (GPC), phosphocreatine (PCr), γ-adrinophosphate (γ-ATP), α-adrinophosphate (α-ATP), diphosphodiester (DPDE), and β-adrinophosphate (β-ATP). Some of the entwined peaks, particularly in the PE/PC, GPE/GPC, and intra- and extra-cellular Pi regions, can be well separated. With the improved NMR perfusion system four MCF7 breast cancer cells drug sensitivity studies were conducted. Drugs with different concentrations were perfused through the NMR containing the cancer cells. The concentrations of the high energy phosphates such as ATP and PCr decreases and the intracellular Pi increases. The GPE and GPC shows a slight increase initially and a decrease later. The changes of phosphorus

metabolism indicate the cells were under stress when first exposed to the drug and later they were overcome by the drug toxicity.

VIII. REFERENCES

1. Michal Neeman, Hadassa Degani Metabolic Studies of Estrogen- and Tamoxifen-treated Human breast Cancer Cells by Nuclear Magnetic Resonance Spectroscopy. Cancer Research 49, 589-594. 1989.
2. Stelling CB, Wang PC, Lieber A, etal, Prototype coil for magnetic resonance imaging of the female breast, Radiology 154(2): 457-62,1985.
3. Harms SE, Flaming DP, Present and Future Role of MR imaging, Syllabus; A categorical Course in Physics Technical Aspects of Breast Imaging RSNA, 1992.
4. Harms SE, Flaming DP, MR imaging of the breast, J. Mag. Res. Imaging 3:277-283, 1993.
5. Harms SE, Flaming DP, Hesley KL, etal, Magnetic Resonance Imaging of the breast, Mag. Res. Quarterly, 8(3):139-155, 1992
6. El Youself SJ, O'Connell DM, Magnetic resonance imaging of the breast, Mag. Res. Annual, 177-195, 1986.
7. Kuelson MH, El Youseif SJ, Goldberg RE, Ballance W, Intracustic Papillary Carcinoma of the breast: mammographic, sonographic and MR appearance with pathologic correlation, J. Comp. Ass. Tomography 11(6):1074-1076, 1987.
8. Partain CL, Kulkarni MV, et al, Magnetic resonance imaging of the breast: Functional T1 and Three-dimensional Imaging, Cardio Vas, Intervent, Radiology 8:292-299, 1986.
9. Santyz GE, Henkelman M, Bronskill M, Spin-locking for magnetic resonance imaging with application to human breast, Mag. Res. Med. 12:25-27, 1989.
10. Adams AH, Brookeman JR, Merickel MB, Breast lesion discrimination using statistical analysis and shape mesures on MRI, Compt. Med. Imaging and Graphics 15(5):339-349, 1991.
11. Harms SE, Flamig DP, Hesley KL, Evans WP, Cheek JH, Ptters GN, Knox SM, Savino DA, Netto GJ, Wells RB, Jones SE. Fat-suppressed Three-dimensional MR Imaging of the Breast,RadioGraphics 13:247-267, 1993.
12. Fischer U, Vosshenrich R, Probst A, Burchhardt H,Grabbe E, Preoperative MR-mammography in diagnosed breast carcinoma, Rofo-Fortschr Geb Rontgenstr Neuen Bildgeb Verfahr 161 (4):300-306 1994.
13. Kuhl C, Specificity of dynamic contrast-enhance MR mammography, Syllabus of Workshop in Breast MR, Soc. Magnet. Reson. p5 June 1995.
14. Aisen, A.M., and Chenevert, T.L. MR spectroscopy: clinical perspective. Radiology 173, 593-599 (1989).
15. Bottomley, P.A. Human in vivo NMR spectroscopy in diagnostic medicine: Clinical tool or research probe? Radiology 170, 1-15 (1989).
16. Daly, P.F., and Cohen, J.S. Magnetic resonance spectroscopy of tumors and potential in vivo clinical applications: A review. Cancer Res. 49, 770-779 (1989).
17. Glickson, J.D. Clinical NMR spectroscopy of tumors. Invest. Radiol. 24, 1011-1016 (1989).
18. den Hollander, J.A., Luyten, P.R., Marien, A.J.H., Segebarth, C.M., Baleriaux, D.F., de beer, R., and Van Ormondt, D. Potentials of quantitative image-localize human ^{31}P nuclear magnetic resonance spectroscopy in the clinical evaluation of intracranial tumors. Mag. Reson. Quarterly 5, 152-168 (1989).
19. Radda, G.K., Rajagopalan, B., and Taylor, D.J. Biochemistry in vivo: An appraisal of

clinical magnetic resonance spectroscopy. Mag. Reson. Quarterly 5, 122-151 (1989).
20. Steen, R.G. Response of solid tumors to chemotherapy monitored by in vivo ^{31}P nuclear magnetic resonance spectroscopy: A review. Cancer Res. 49, 4075-4085 (1989).
21. Vaupel, P., Kallinowski, F., and Okunieff P. Blood flow, oxygen and nutrient supply, and metabolic microenvironment of human tumors: A review. Cancer Res. 49, 6449-6465 (1989).
22. Negendank W, Studies of Human Tumors by MRS : a Review, NMR Biomed. 5:303-324 1992.
23. Barfuss, H. et al. In vivo Magnetic Resonance Imaging and Spectroscopy of Humans with a 4 T Whole Body Magnet. NMR in Biomed. 3:31-45, 1989.
24. Hetherington, HP, Pan, JW, Mason GF, et al. High Resolution ^{1}H Spectroscopic imaging of Human Brain at High Field Quantitative Evaluation of Gray and White Matter Metabolite Differences, 12th Ann. Meeting Soc. Mag. Res. Med. p. 127, 1993.
25. Posse, S., Cuenod, CA, Balaban, RS, Le Bihan, D. Anomalous Transverse Relaxation in ^{1}H Spectroscopy in Human Brain at 4 Tesla. 12th Ann. Meeting Soc. Mag. Res. Med. p. 371, 1993.
26. Ugurbil, K. Insensitive Adiabatic RF Pulses. Syllabus of 12th Ann. Meeting Soc. Mag. Res. Med. 195-202, 1993.
27. W.A. Edelstein, G.H. Glover, C.J. Hardy, R.W. Redington. Magn. Reson. Med. 3, 604, 1986.
28. R.D. Black, T.A. Early, P.B. Roemer, O.M. Mueller, A Mogro Campero, L.G. Turner, G. A. Johnson. A High-Temperature Superconducting Receiver for NMR Microscopy. Science 259:793-795, 1993.
29. D.I. Hoult and R.E. Richards, "The signal-to-noise ratio of the nuclear magnetic resonance experiment," J.Mag.Res. 24, 71-85, 1976.
30. Black R.D., P.B. Roemer, W.A. Edelstein, S.P. Souza, A. Mogro Campero, L.G. Turner, Scaling Laws and Cryogenic Probes for NMR Microscopy in Proceedings of the Tenth Annual Meeting of the Soc. Magn. Reson. Med. San Fransisco, CA, August 10-16, 1991.
31. Vogl, T., Peer, F., Schedel, H., Reiman, V., Holtmann, S., Rennschmid, C., Sauter, R., and Lesner, J. ^{31}P-spectroscopy of head and neck tumors - Surface coil technique. Magn. Reson. Imaging 7, 425-435 (1989).
32. Koutcher, J.A., Ballon, D., Graham, M., Healey, J.H., Casper, E.S., Heelan, R., and Gerweck, L.E. ^{31}P NMR spectra of extremity sarcomas: diversity of metabolic profiles and changes in response to chemotherapy. Magn. Reson. Med. 16, 19-34 (1990).
33. Shinkwin, M.A., Lenkinski, R.E., Daly, J.M., Zlatkin, M.B., Frank, T.S., Holland, G.A., and Kressel, H.Y. Integrated magnetic resonance imaging and phosphorous spectroscopy of soft tissue tumors. Cancer 67, 1849-1858 (1991).
34. Glaholm, J., Leach, M.O., Collins, D.J., Mansi, J., Sharp, J.C., Madden, A., Smith, I.E., and McCready, V.R. In vivo ^{31}P magnetic resonance spectroscopy for monitoring treatment response in breast cancer. Lancet I, 1326-1327 (1989).
35. Ng, T.C., Grundfest, S., Vijayakumar, S., Baldwin, N.J., Majors, A.W., Karalis, I., Meaney, T.F., Shin, K.H., Thomas, F.J., and Tubbs, R. Therapeutic response of breast carcinoma monitored by ^{31}P MRS in situ. Magn. Reson. Med. 10, 125-134 (1989).
36. Twelves, C.J., Lowry, M., Porter, D., Graves, P., Smith, M.A., and Richards, M.A. ^{31}P MR spectroscopy of breast cancer in vivo: metabolite characteristics and influence of estrogen receptor status and tumor grade. Soc. Mag. Res. Med. Abstr., p. 1216 (1990).

37. Kalra, R., Hands, L., Styles, P., Wade, K., Greenall, M., Smith, K., Harris, A., and Radda, G.K. Localized ^{31}P spectroscopy of human breast cancer correlations of phosphomonoester and phosphodiester with epiderman growth factor expresion. Soc. Mag. Res. Med. Abstr., p. 1217 (1990).
38. Redmond, O.M., Stack, J.P., O'Connor, N.G., Codd, M.B., and Ennis, J.T. In vivo phosphorous ^{31}P magnetic resonance spectroscopy of normal and pathological breast tissue. Br. J. Radiology 65, 210-216 (1991).
39. Mimnaugh, E.G., Fairchild, C.R., Fruehauf, J.P., and Sinha, B.K. Biochemical and pharmacological characterization of MCF-7 drug-sensitive and Adr^R multidrug resistant human breast tumor xenografts in athymic nude mice.Bichem. Pharmacol. 42:391-402, 1991.
40. Cohen, J.S., Lyon, R.C., Chen, C., Faustino, P.J., Batist, G., Shoemaker, M., Rubalcaba, E. and Cowan, K.H. Differences in phosphate metabolite levels in drug-sensitive and resistant human breast cancer lines determined by ^{31}P magnetic resonance spectroscopy. Cancer Res. 56:4087-4090, 1986.
41. Garwood, M. Introduction to Basic Principles of Spectral Localization. Syllabus,11th Ann. Meeting, Soc. Mag. Res. Med. p. 222-231, 1992.
42. R.J. Ordidge, M.R. Bendall, R.E. Gordon, and A. Connelly, MAgnetic resonance in biology and medicine (Govil, Khetrapal, and Saran, Eds.), p.387, Mcgraw-Hill, New Delhi, 1985.
43. Bottomley PA, Hardy CJ, Roemer RB, Weiss RG, Problems and expediencies in human 31P spectroscopy, The definition of localized volumes, dealing with saturation and the technique-dependence of quantification NMR in Biomedicine, 2:284-289, 1989.
44. Granot J, Selective volume excitation using stimulated echoes (VEST), Applications to spatially localized spectroscopy and imaging, J. Magn. Res. 70,488-492 (1986).
45. Kimmich R and D. Hoepfel, Volume selective multipulse spin-echo spectroscopy, J. Magn. Reson. 72, 379 (1987).
46. Frahm J, K.D. Merboldt, and W. Hanicke, Localized proton spectroscopy using stimulated echoes, J. Magn. Reson. 72, 502 (1987).
47. Ordidge RJ, A. Connelly, and J.A.B. Lohman, Image selected in vivo spectroscopy (ISIS), A new technique for spatially-selective NMR spectroscopy, J. Magn. Reson. 66, 283 (1986).

IX. Appendices

Cells Perfusion System For NMR Study

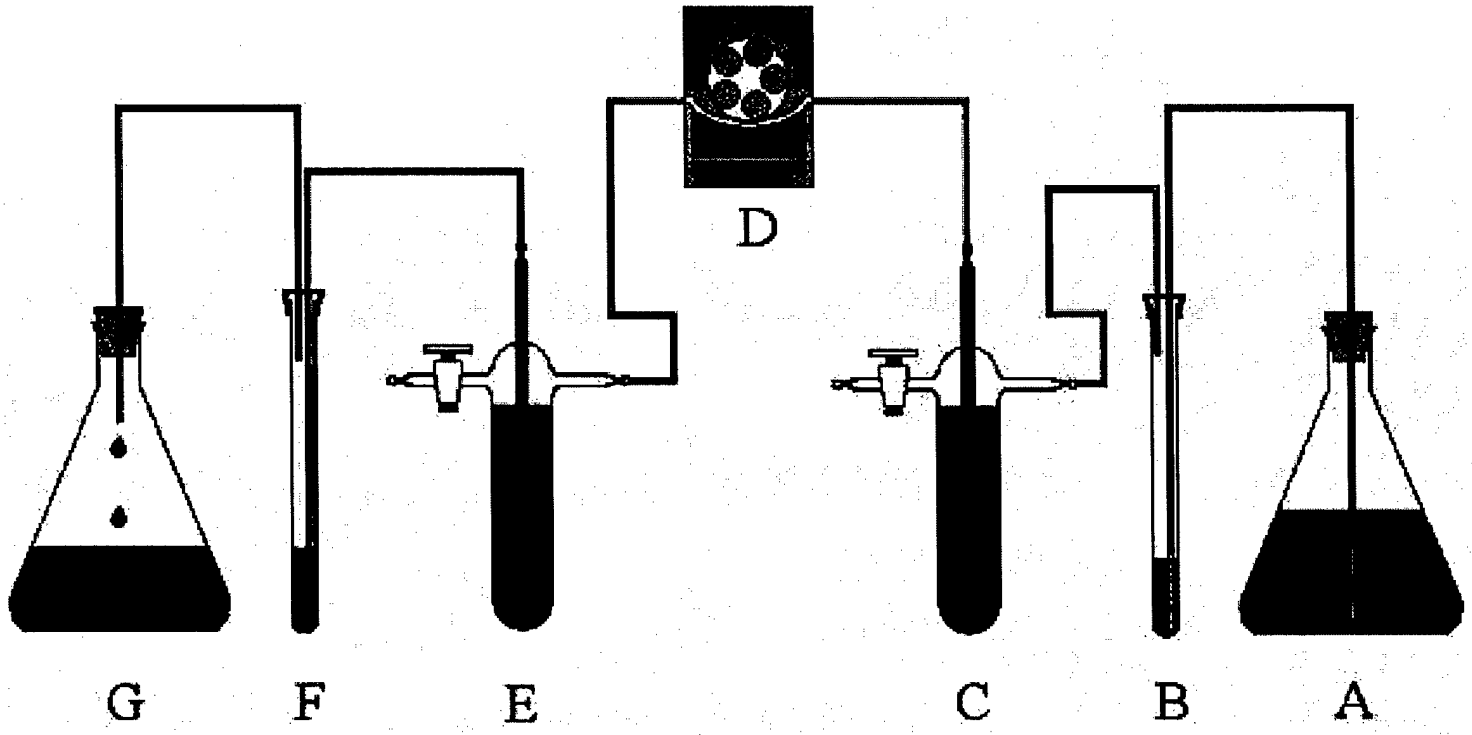

Figure 1. An improved cell perfusion system (A) medium reservoir (B) gas release inducer (C) gas trap (D) pump (E) gas trap (F) NMR tube (G) waste collector

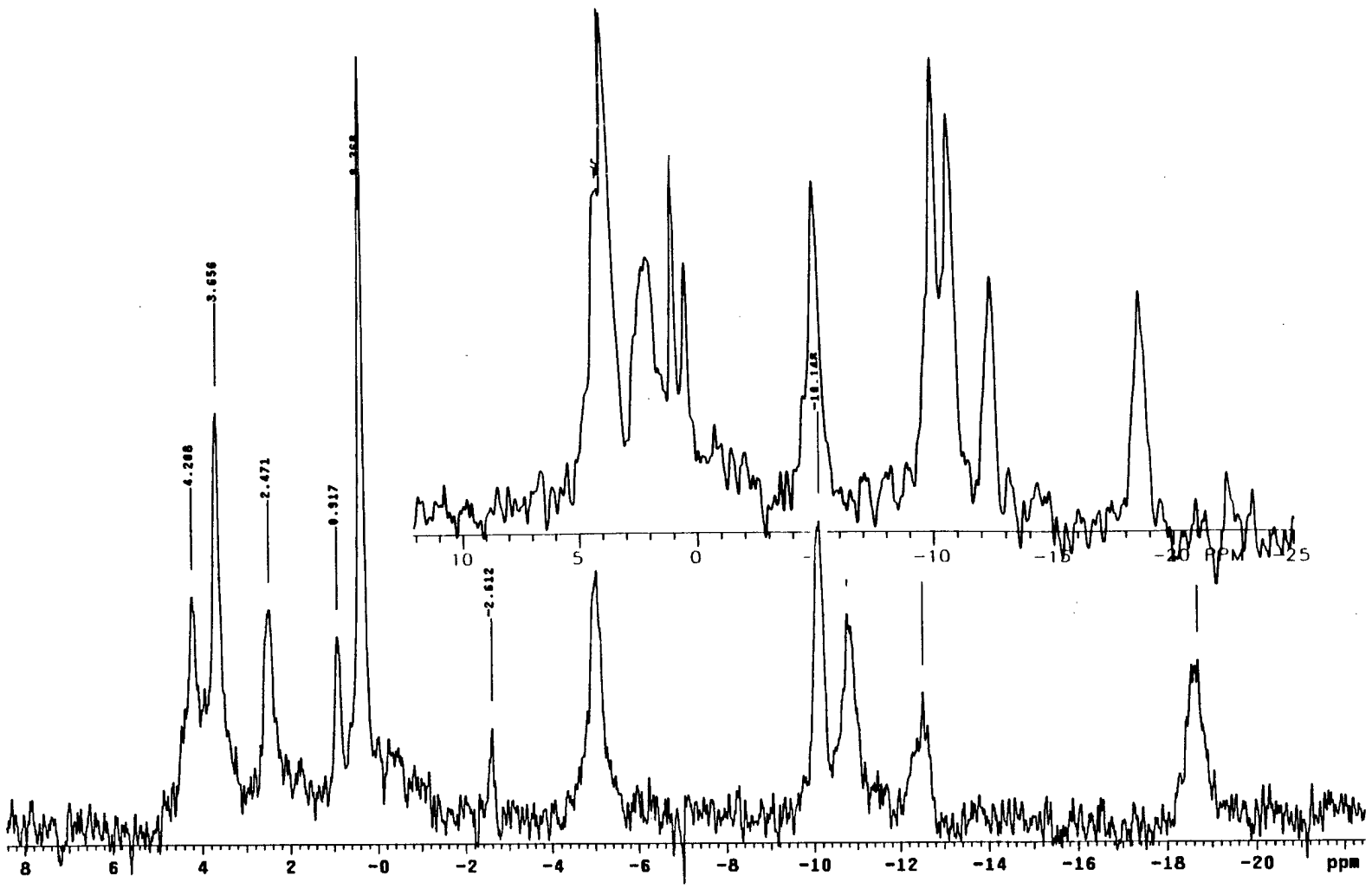

Figure 2. A ^{31}P NMR spectrum of a wild type MCF7 breast cancer cells (10^8 cells) embedded in agarose gel threads. Phosphorus metabolites, including phosphoethanolamine (PE, 4.21 ppm), phosphocholine (PC, 3.66), inorganic phosphate (Pi, 2.47), glycerophosphoethanolamine (GPE, 0.92), glycerophosphocholine (GPC, 0.37) phosphocreatine (PCr, -2.61), γ-adrinophosphate (γ-ATP, -5.05), α-adrinophosphate (α-ATP, -10.15), diphosphodiester (DPDE, -10.78, -12.53), and β-adrinophosphate (β-ATP, -18.70), can be easily identified. The spectrum is an accumulation of 1800 transients and the repetition time is 2 seconds. The signal-to-noise ratio is significantly better than the results in the previous report (see the insert). The line width of the γ-ATP peak is 50 Hz.

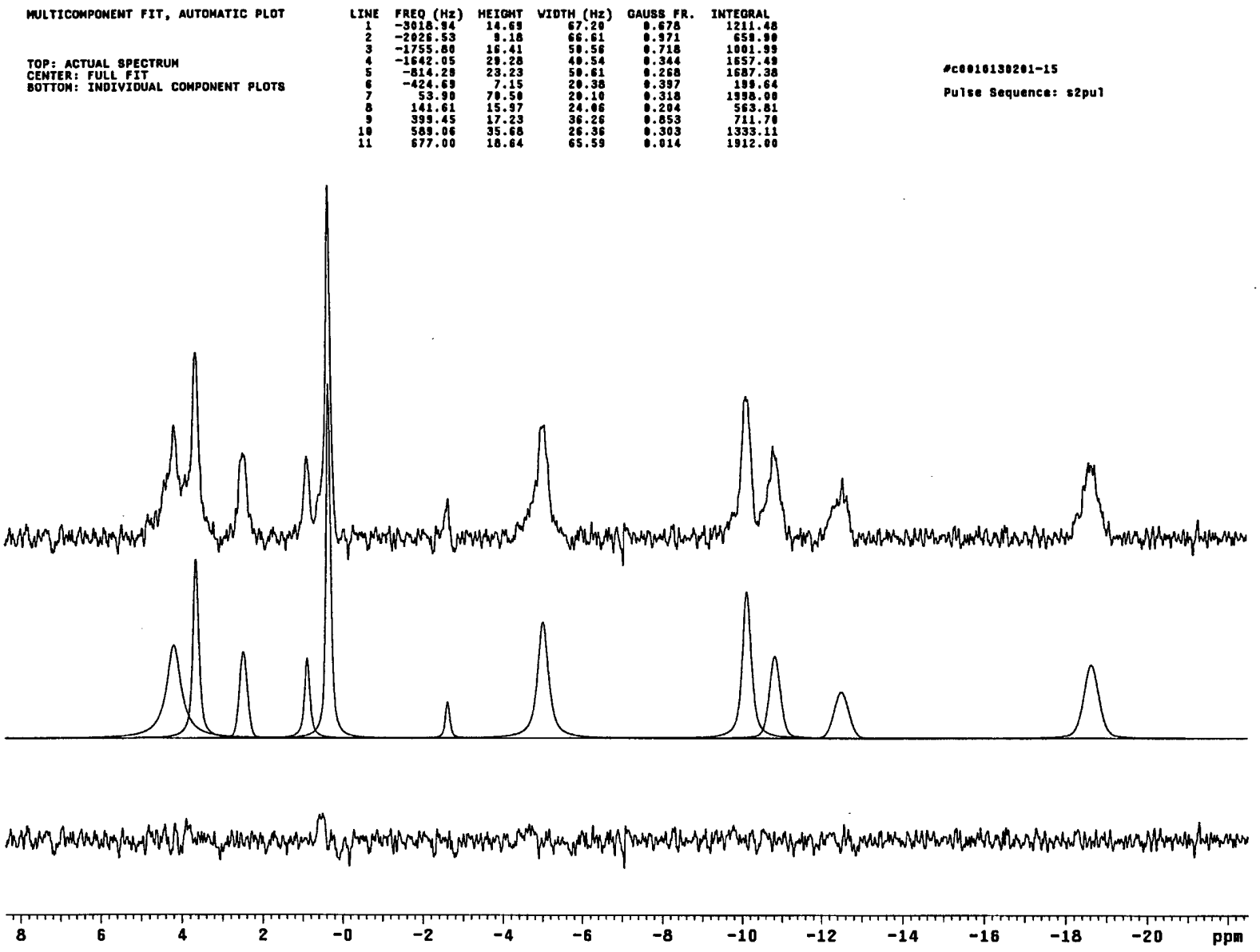

Figure 3. (A) Deconvolution of the ^{31}P NMR spectrum from the Figure 2. (B) Individual phosphorus metabolite peaks that have been separated from the original spectrum. The individual peak-heights and the integrals under the peaks can be derived and are listed in the inserted table. (C) The differences between the original spectrum and the fitted curve.

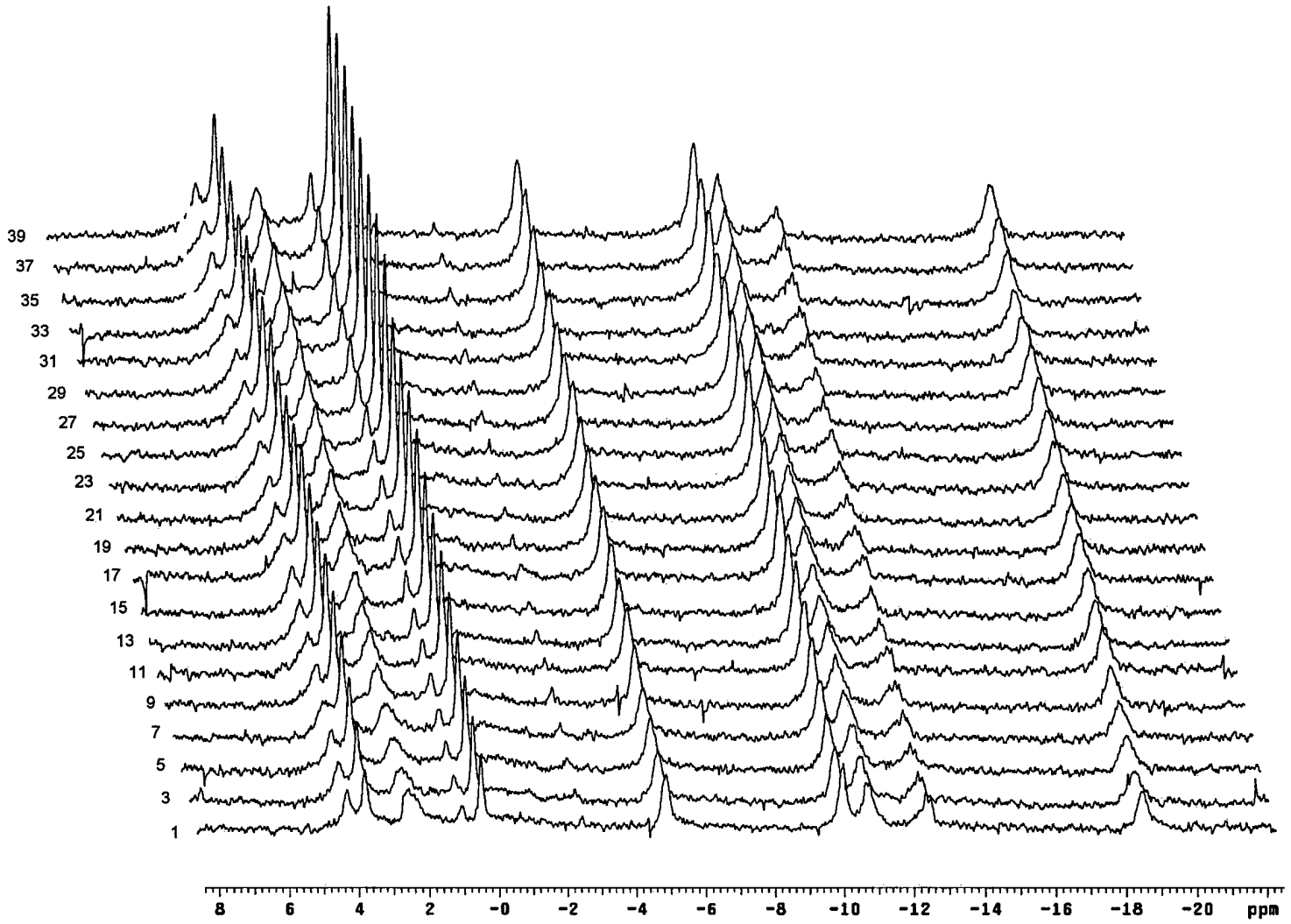

Figure 4. **A long term in vivo ^{31}P NMR spectroscopy study of MCF7 breast cancer cells. A series of 47 ^{31}P spectra over 5 days were obtained. Each spectrum is an accumulation of 3 hours, 5370 transients and 2 seconds repetition time. The changes of each phosphorus metabolites can be easily studied. During this time, PC, GPE and GPC increases while other phosphorus metabolites stay constant.**

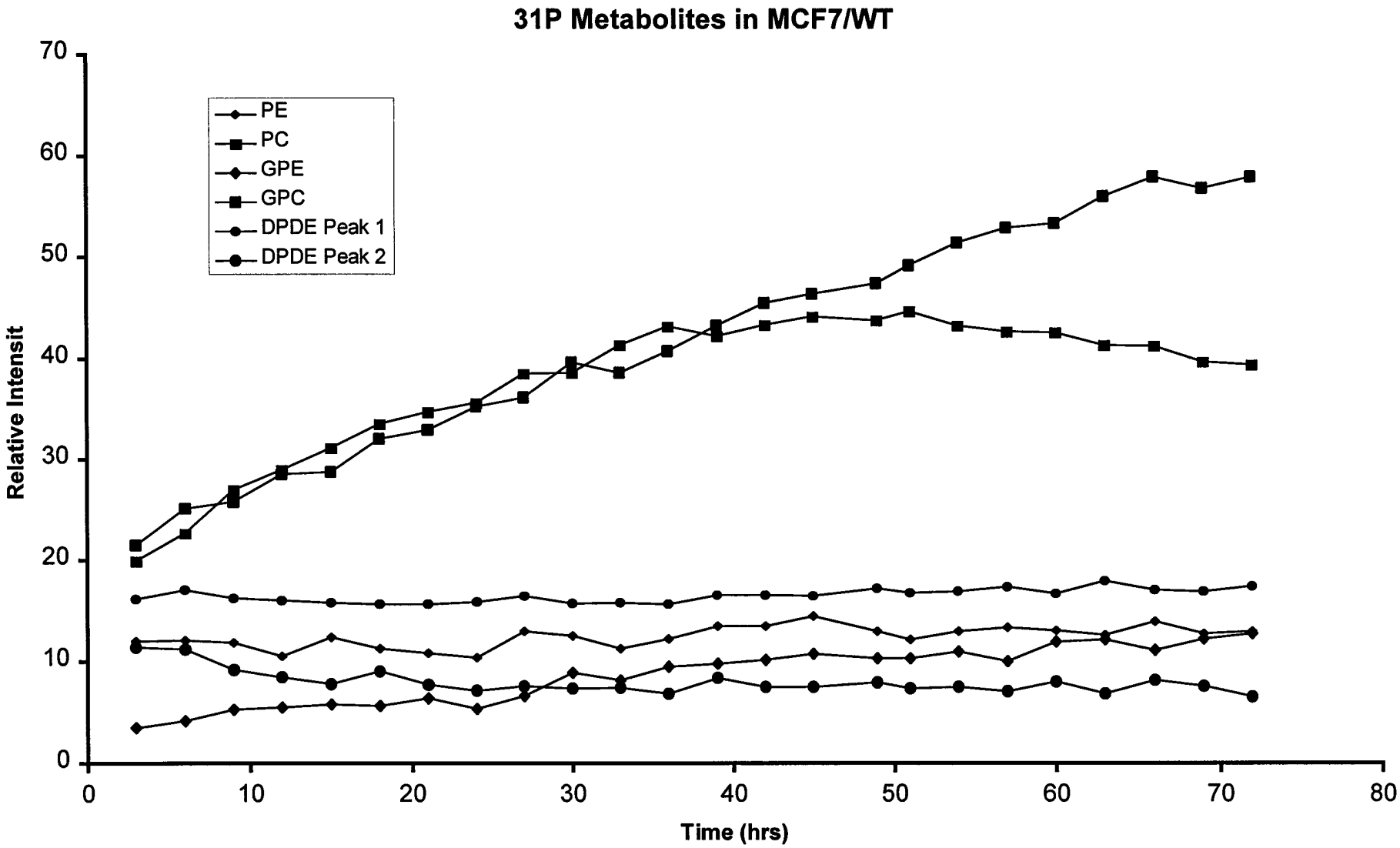

Figure 5A. Changes of individual phosphorus metabolites of MCF7/WT (wild type) cells over first 72 hours in a long in vivo study described in Figure 4. This figure contains only 6 out of 11 phosphorus metabolites: PE, PC, GPC and DPDE. The absolute concentrations of the metabolites are plotted as functions of time.

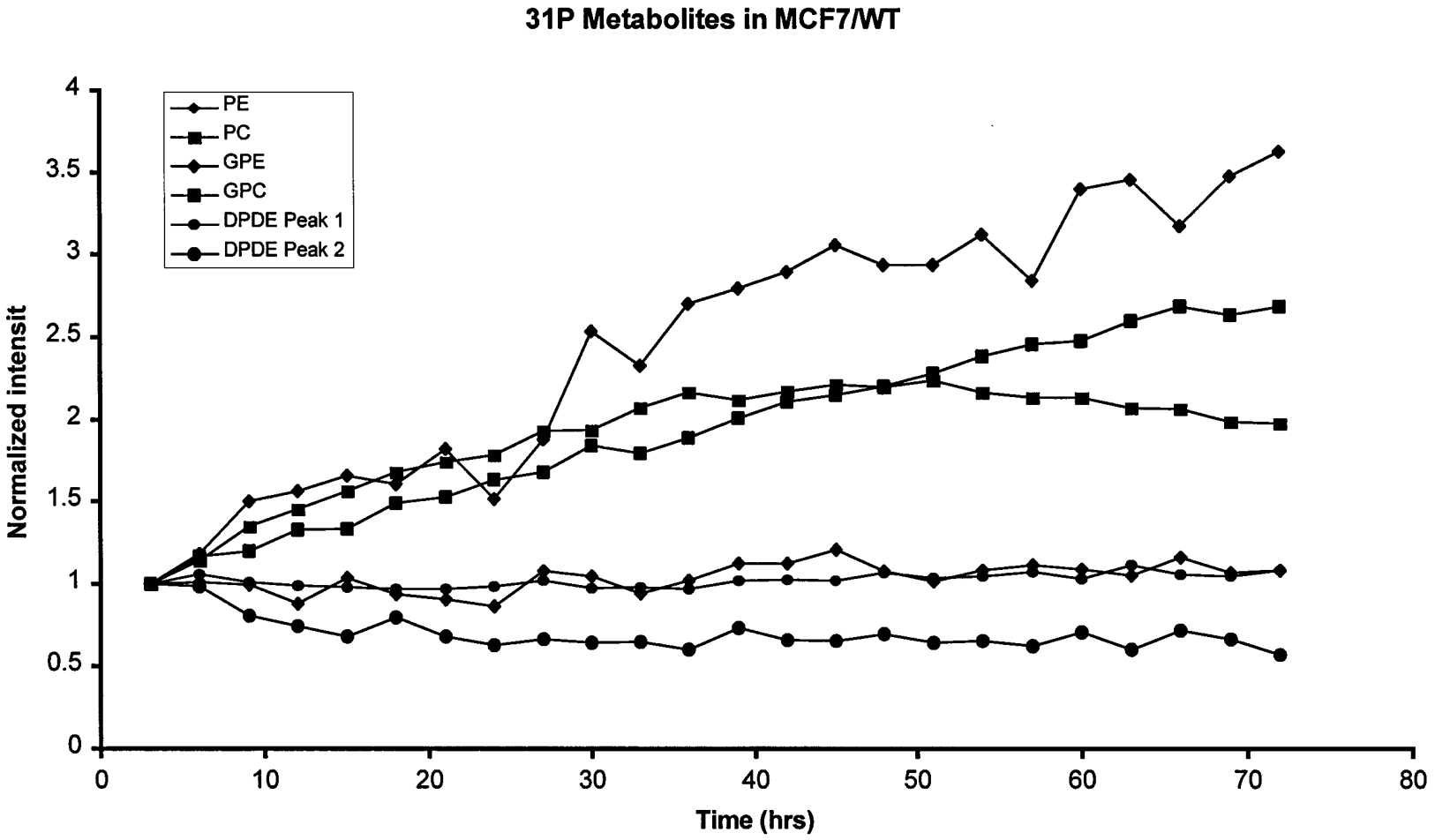

Figure 5B. Changes of individual phosphorus metabolites of MCF7/WT (wild type) cells over first 72 hours in a long in vivo study described in Figure 4. This figure contains only 6 out of 11 phosphorus metabolites: PE, PC, GPC and DPDE. The relative intensities of these metabolites are compared with their original concentrations. During the first 72 hours, GPE and GPC continuously increase while PE and DPDE remains constant. PC increases initially and it approaches a plateau later. The increases of GPE and GPC indicate the cell proliferation.

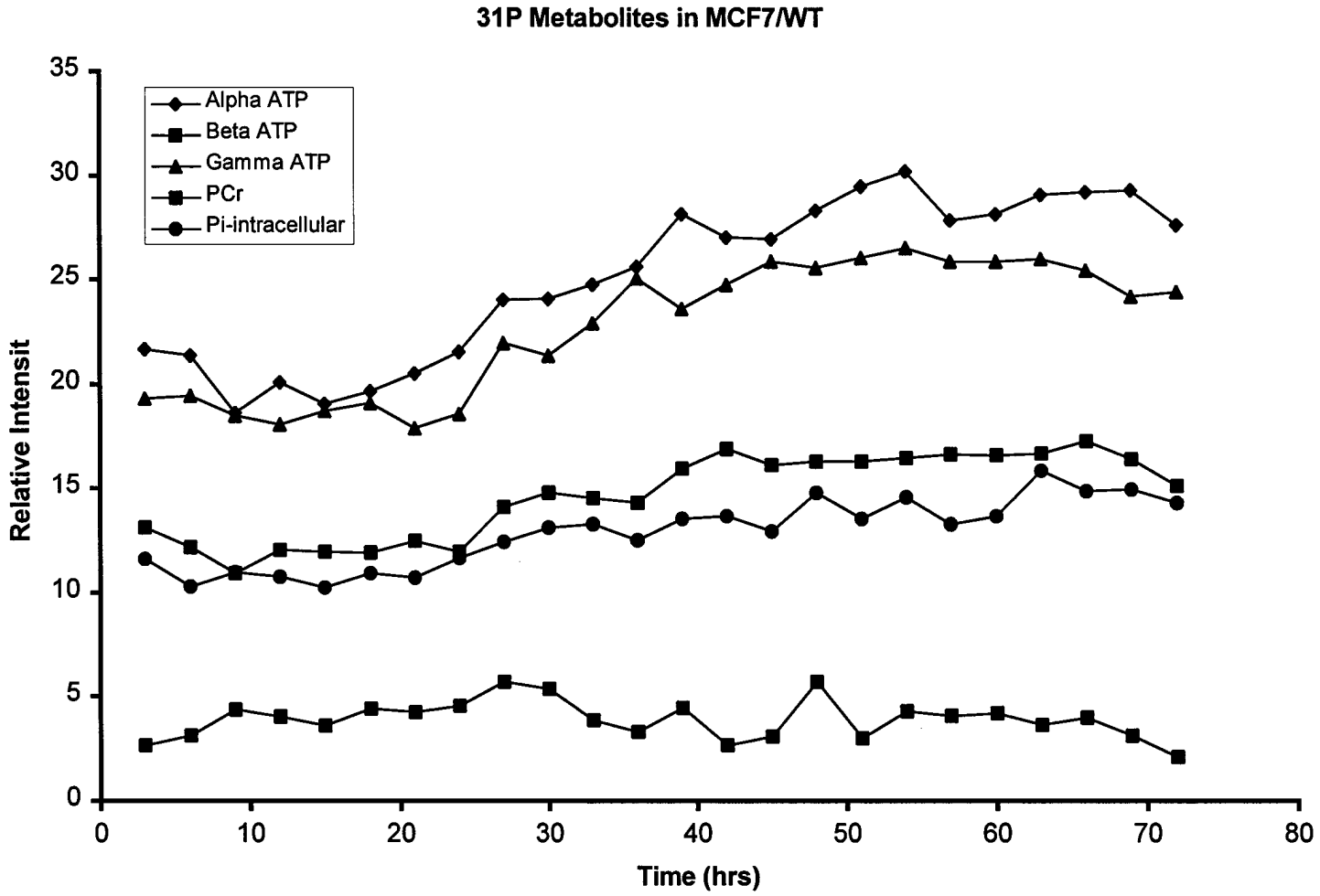

Figure 6A. Changes of individual phosphorus metabolites of MCF7/WT cells over first 72 hours from a long in vivo study described in Figure 4. The concentrations of another five phosphorus metabolites α-ATP, β-ATP, γ-ATP, PCr, and Pi are plotted as functions of time.

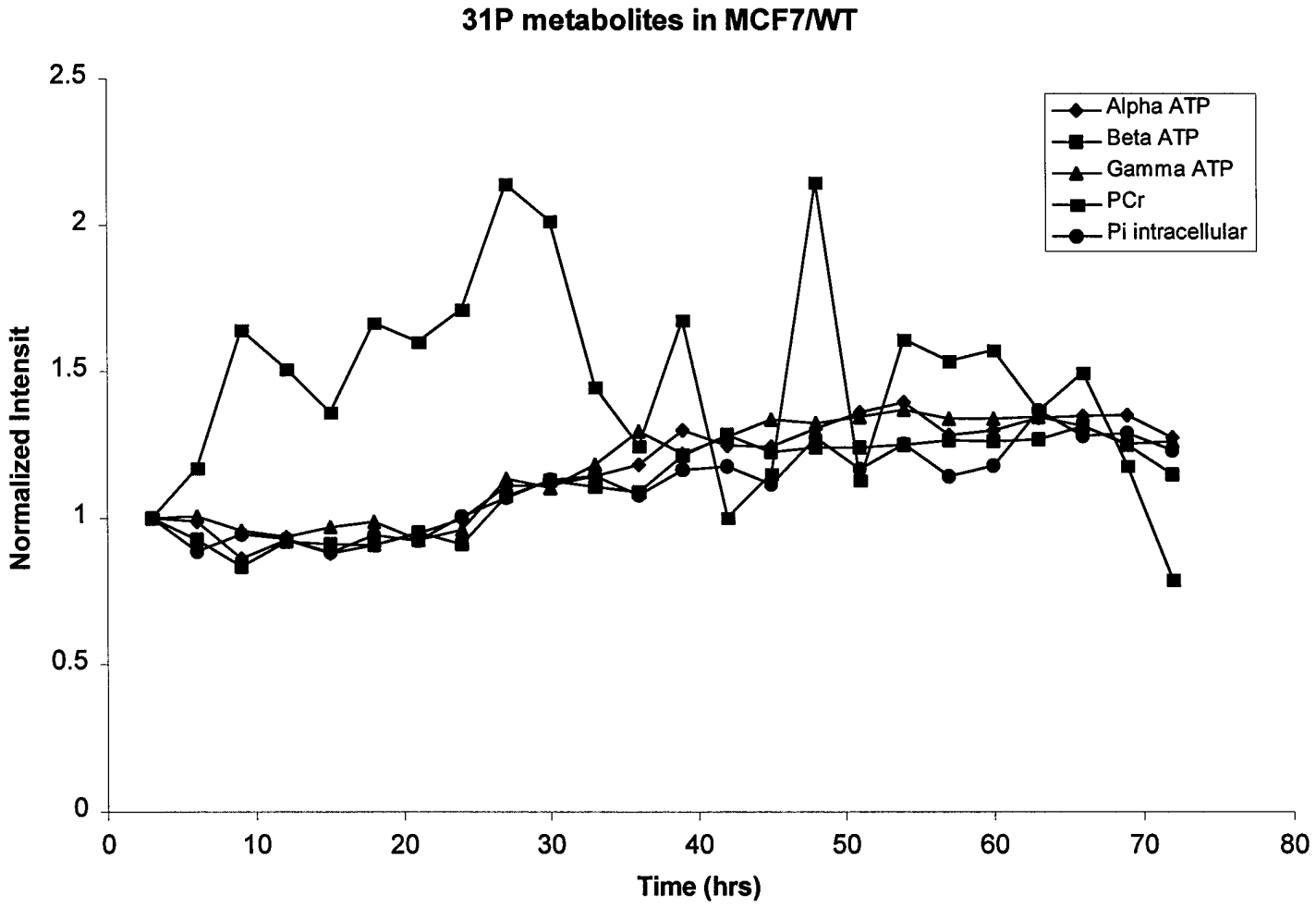

Figure 6B. Changes of individual phosphorus metabolites of MCF7/WT cells over first 72 hours from a long in vivo study described in Figure 4. The concentrations of another five phosphorus metabolites α-ATP, β-ATP, γ-ATP, PCr, and Pi are plotted as functions of time. The relative intensities of each metabolite are plotted relative to their original concentrations. During the course of study ATP and Pi continuously grow. PCr remains low concentration.

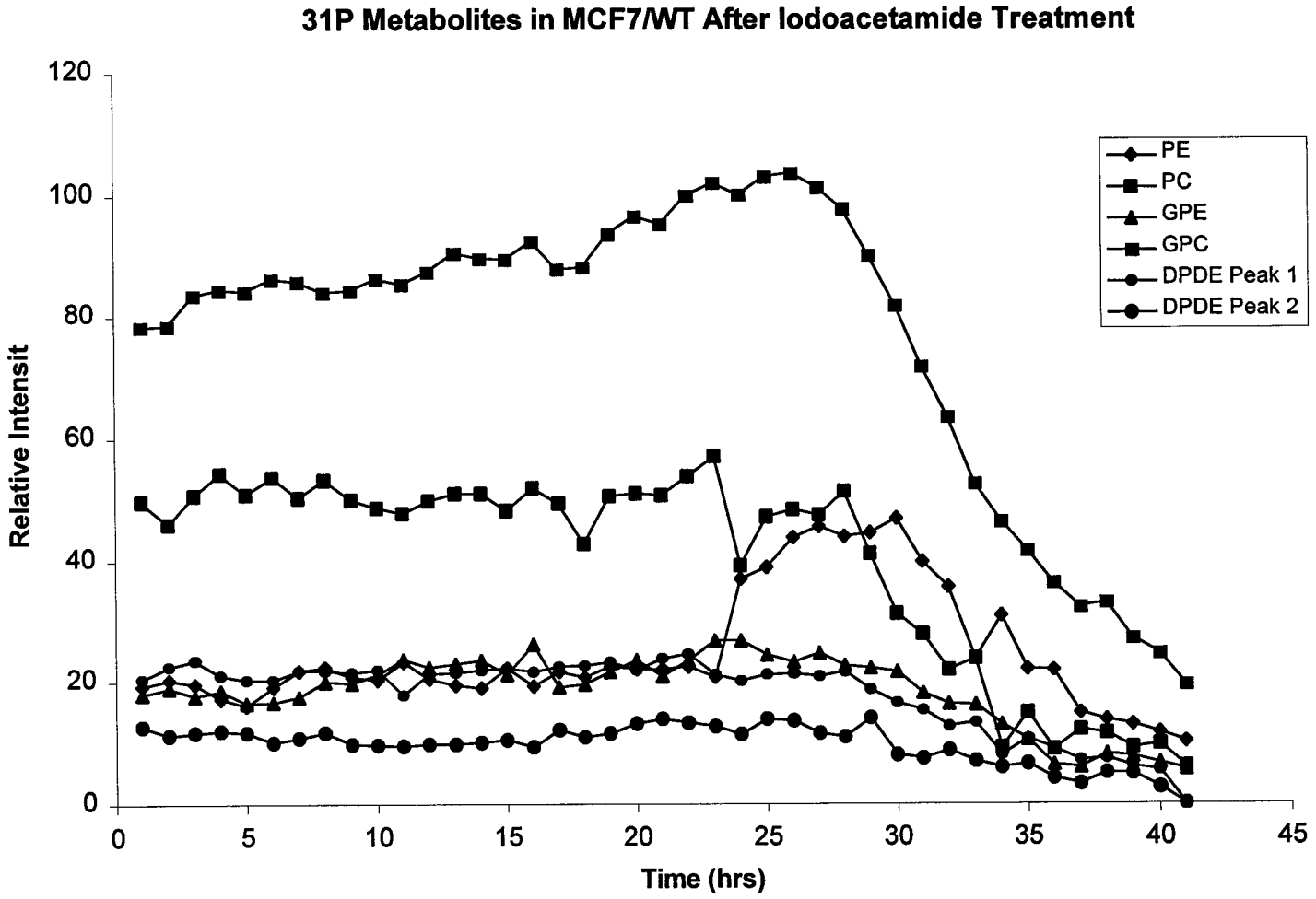

Figure 7A. **A drug sensitivity study. 10^8 MCF7/WT breast cancer cells embedded in the agarose gel perfused with growth medium were used. Forty-two ^{31}P NMR spectra were taken every hour. Each spectrum contains 1700 transients with 1 second repetition time. After 17 hours baseline study, 1mM iodoacetamide was added in the perfused medium. All the phosphorus metabolites concentrations are plotted as functions of time. Six metabolites are in this figure and the other five metabolites are in Figure 8. The concentration changes of the PE, PC, GPE, GPC and DPDE are plotted as function of time.**

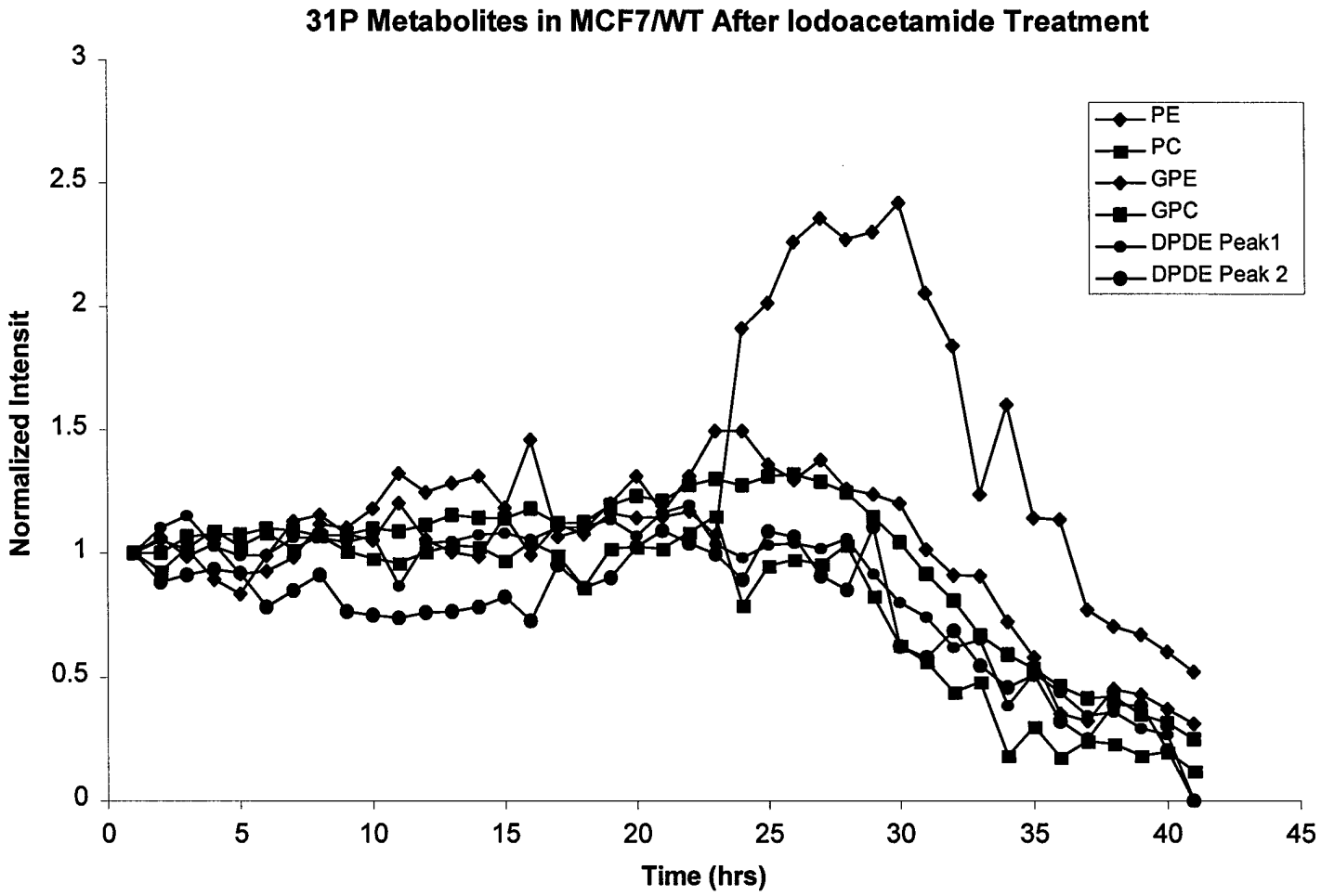

Figure 7B. **A drug sensitivity study. 10^8 MCF7/WT breast cancer cells embedded in the agarose gel perfused with growth medium were used. Forty-two ^{31}P NMR spectra were taken every hour. Each spectrum contains 1700 transients with 1 second repetition time. After 17 hours baseline study, 1mM iodoacetamide was added in the perfused medium. All the phosphorus metabolites concentrations are plotted as functions of time. Six metabolites PE, PC, GPE, GPC and DPDE are in this figure and the other five metabolites are in Figure 8. The relative concentration changes to the beginning of the study are plotted as functions of time. After perfusion with iodoacetamide, PE increases dramatically and then decreases. GPE and GPC show slightly increases initially and decreases afterwards. DPDE shows continuous decreases.**

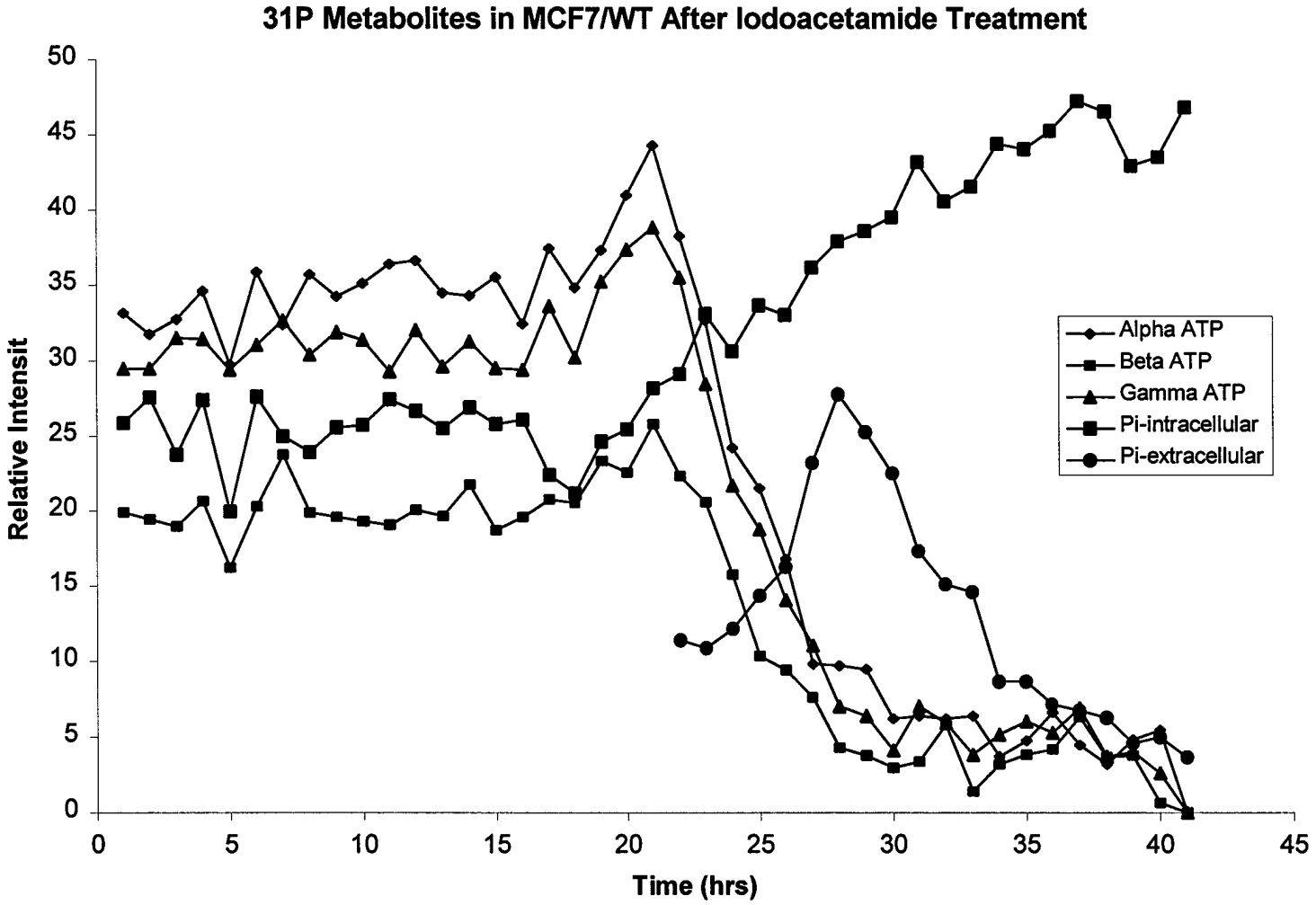

Figure 8A. Concentrations of phosphorus metabolites before and after drug treatment. This figure contains the other five phosphorus metabolites: α-ATP, β-ATP, γ-ATP, intra- and extra- cellular Pi. The absolute concentrations are plotted as function of time.

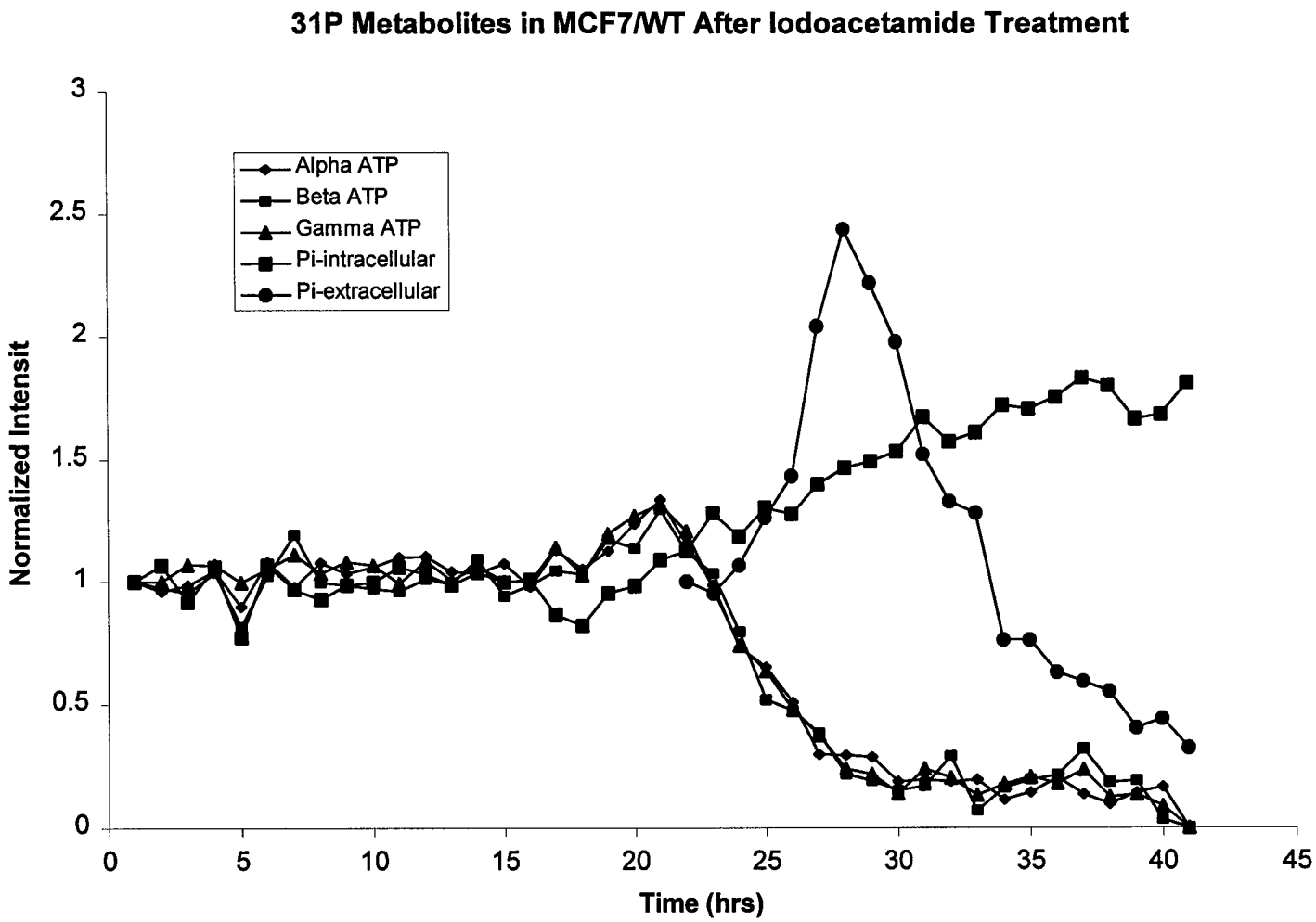

Figure 8B. Concentrations of phosphorus metabolites before and after drug treatment. This figure contains the other five phosphorus metabolites: α-ATP, β-ATP, γ-ATP, intra- and extra- cellular Pi. The relative concentration changes are compared against the initial concentration. After perfusion with 1mM iodoacetamide at the 17th hour, ATP increases slightly and then decreases. The intracellular Pi continuously increases. The extracellular Pi appears after the drug perfusion and increases few hours before it disappears due to perfusion.

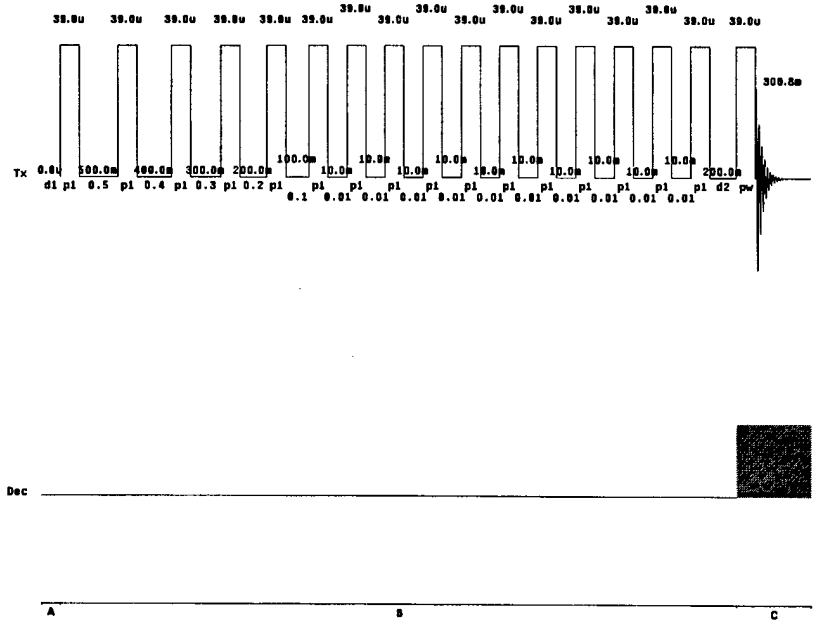

Name of Compound		Peak (ppm)	T1 (sec)	SD
Phosphoethanolamine(PE)		4.156	2.65	0.511
Phosphocholine (PC)		3.646	4.69	0.329
Inorganic Phosphate (intracellular)		2.631	5.36	1.031
Glycerolphosphoethanolamine(GPE)		0.892	>12	
Glycerolphosphocholine (GPC)		0.334	7.04	0.886
Phosphocreatine (PCr)		-2.633	3.04	1.30
Gamma ATP		-5.045	0.573	0.119
Alpha ATP		-10.132	0.606	0.084
Diphosphodiester Peak 1 (DPDE 1)		-10.844	1.45	0.112
Diphosphodiester Peak 2 (DPDE 1)		-12.557	1.60	0.271
Beta ATP		-18.612	0.383	0.055

Figure 9. T1 relaxation time measurement. The NMR T1 relaxation times of all the phosphorus metabolites of MCF7 breast cancer cells were measured with the improved NMR perfusion system. (A) A saturation recovery technique is used. A series of 16 RF pulses flips the magnetization to a horizontal plane first. It follows by a 90^0 RF pulse and data acquisition period. (B) A list of measured T1 relaxation times for each phosphorus metabolites. The T1 values vary from 0.38 seconds for β-ATP and longer than 12 seconds for GPE.